

# X(3872) and its production at hadron colliders

Ce Meng<sup>a,\*</sup>, Hao Han<sup>a,†</sup> and Kuang-Ta Chao<sup>a,b,‡</sup>

(a) Department of Physics and State Key Laboratory of Nuclear Physics and Technology, Peking University, Beijing 100871, China

(b) Center for High Energy physics, Peking University, Beijing 100871, China

(Dated: April 25, 2013)

We evaluate the production cross sections of  $X(3872)$  at the Tevatron and LHC at NLO in  $\alpha_s$  within the framework of NRQCD factorization by assuming that the short distance production proceeds dominantly through its  $\chi'_{c1}$  component. The outcomes of the fits to the CMS  $p_T$  distribution can well account for the CDF data, and are consistent with the value of  $k = Z_{c\bar{c}} \cdot Br(X \rightarrow J/\psi \pi^+ \pi^-)$  constrained by the B meson decay data. In comparison, the molecule dominant production mechanism for  $X(3872)$  is inconsistent with both the  $p_T$  distributions and the total cross sections of the CMS and CDF data.

PACS numbers: 12.38.Bx, 13.25.Gv, 14.40.Pq

*Introduction.*— The hidden-charm state  $X(3872)$  was first discovered by Belle Collaboration in the  $J/\psi \pi^+ \pi^-$  invariant mass spectrum of  $B^+ \rightarrow J/\psi \pi^+ \pi^- K^+$  decay [1], and confirmed by CDF [2], D0 [3] and BaBar [4] Collaborations soon after. The closeness of the mass  $m_X = 3871.68 \pm 0.17$  MeV [5] to the  $D^0 \bar{D}^{*0}$  threshold led many authors to speculate that the  $X$  is a  $D^0 \bar{D}^{*0}$  molecule [6]. (For recent reviews of  $X(3872)$ , see Ref. [7])

However, with the tiny binding energy  $E_b = (m_{D^0} + m_{\bar{D}^{*0}}) - m_X = 0.142 \pm 0.220$  MeV [8], it is difficult to imagine that such a loosely bound state can have a large prompt production rate (i.e. not from  $B$  decays) in  $p\bar{p}$  collision. In addition, D0 Collaboration [3] found that the behavior of  $X(3872)$  production in  $p\bar{p}$  collision is very similar to that of  $\psi'$ , such as the cross section  $p_T$  distribution. In view of these, we proposed that the  $X(3872)$  is a mixed state of  $\chi_{c1}(2P)$  ( $\chi'_{c1}$ ) and  $D^0 \bar{D}^{*0}$  continuum [9]. The two components both are substantial and may play different roles in the dynamics of  $X(3872)$ : the short distance (the  $b$ - and  $hadro$ -) production and the quark annihilation decays of  $X$  proceed dominantly through the  $\chi'_{c1}$  component; while the  $D^0 \bar{D}^{*0}$  component is mainly in charge of the hadronic decays of  $X(3872)$  into  $DD\pi, DD\gamma$  as well as  $J/\psi \rho$  and  $J/\psi \omega$ . Based on the calculation for the ratio  $\frac{Br(B \rightarrow \chi'_{c1} K)}{Br(B \rightarrow \chi_{c1} K)}$ , we estimated that  $Br(B \rightarrow \chi'_{c1} K) = (2-4) \times 10^{-4}$  [9], which is consistent with the experimental constraints on  $Br(B \rightarrow X(3872) K)$  renormalized by  $Z_{c\bar{c}}$ , where  $Z_{c\bar{c}}$  is the probability of the  $\chi'_{c1}$  component in the  $X(3872)$ . We also calculated the  $X$  decays into  $J/\psi \rho$  and  $J/\psi \omega$  through rescattering of the intermediate states, i.e. the  $D^0 \bar{D}^{*0}$  component, and this may account for the observed large isospin violation [10]. The closeness of the mass of  $X(3872)$  to the  $D^0 \bar{D}^{*0}$  threshold may be explained by the S-wave coupling between the  $J^{PC} = 1^{++} c\bar{c}$  component ( $\chi'_{c1}$ ) and the  $D^0 \bar{D}^{*0}$  component, which induces a sharp spectral

density and lowers the "bare" mass of  $\chi'_{c1}$  towards the  $D^0 \bar{D}^{*0}$  threshold [11].

As for the prompt production of  $X$  in  $p\bar{p}$  collision, Suzuki [12] also pointed out that the molecule assumption can hardly be consistent with the CDF measurement, based on an estimation of the wave function at the origin for the molecule. More explicit calculations given by Bignamini *et al.* [13] set the upper bound of the cross section of  $X$  as a  $D^0 \bar{D}^{*0}$  molecule to be 0.085 nb, which is smaller than the experimental lower bound

$$\sigma(p\bar{p} \rightarrow X) \times Br(X \rightarrow J/\psi \pi^+ \pi^-) = 3.1 \pm 0.7 \text{ nb.} \quad (1)$$

by about two orders of magnitude.

Artoisenet and Braaten [14] suggested that the  $D\bar{D}^*$  rescattering effects could enhance the molecule production cross section to values consistent with CDF data if one choose the upper bound of the relative momentum of  $D\bar{D}^*$  rescattering to be  $3m_\pi$  or more. With NRQCD factorization [15] at leading order (LO) and with the matrix element extracted from the CDF data of  $X(3872)$ , they also made predictions for the molecule production cross section at LHC, which is about 3 to 4 times larger than the recent LHCb [16] and CMS [17] data.

In our view, with the  $\chi'_{c1} - D^0 \bar{D}^{*0}$  mixing model, one can naturally understand the prompt production of  $X(3872)$  at the Tevatron and LHC: the  $X(3872)$  production actually proceeds via the  $\chi'_{c1}$  component and shares similar behavior to that of  $\psi'$ . In this letter, we will study the prompt production of  $X(3872)$  at next-to-leading order (NLO) in NRQCD, and compare our results with the molecule model on both the total cross sections and  $p_T$  distributions. We will also discuss the constraints on the value of  $Z_{c\bar{c}}$  indicated by our calculation.

*Prompt  $X(3872)$  production in NRQCD.*—In the  $\chi'_{c1}$  dominant production mechanism, the inclusive cross section of  $X$  in the  $J/\psi \pi^+ \pi^-$  mode can be expressed as

$$d\sigma(pp \rightarrow X(J/\psi \pi^+ \pi^-)) = d\sigma(pp \rightarrow \chi'_{c1}) \cdot k, \quad (2)$$

where  $p$  is either a proton or an antiproton and  $k = Z_{c\bar{c}} \cdot Br_0$  with  $Br_0 = Br(X \rightarrow J/\psi \pi^+ \pi^-)$ . The feed-down contributions from higher charmonia (e.g.  $\psi(3S)$

\*Electronic address: mengce75@pku.edu.cn

†Electronic address: unknowndear@163.com

‡Electronic address: ktchao@pku.edu.cn

are negligible for the prompt production of  $X(3872)/\chi'_{c1}$ , so here "prompt" is almost equal to "direct", and the cross section of  $\chi'_{c1}$  in (2) can be evaluated in NRQCD factorization, which is given by

$$d\sigma(pp \rightarrow \chi'_{c1}) = \sum_n d\hat{\sigma}((c\bar{c})_n) \frac{\langle \mathcal{O}_n^{\chi'_{c1}} \rangle}{m_c^2 L_n} \quad (3)$$

$$= \sum_{i,j,n} \int dx_1 dx_2 G_{i/p} G_{j/p} d\hat{\sigma}(ij \rightarrow (c\bar{c})_n) \langle \mathcal{O}_n^{\chi'_{c1}} \rangle,$$

where  $G_{i,j/p}$  are the parton distributions functions (PDFs) of  $p$ , and the indices  $i, j$  run over all the partonic species. The matrix element  $\langle \mathcal{O}_n^{\chi'_{c1}} \rangle$  is marked by "n", which denotes the color, spin and angular momentum of the intermediate  $c\bar{c}$  pair. Here we will evaluate the cross section at NLO in  $\alpha_s$  and LO in  $v$  (the relative velocity of  $c\bar{c}$  in the rest frame of  $\chi'_{c1}$ ), therefore, only  $n = {}^3P_1^{[1]}$  and  ${}^3S_1^{[8]}$  are present here.

Since  $\chi_{c1}(1P)$  and its radial excitation  $\chi'_{c1}$  share the same quantum number, they are physically alike. For the purpose of comparison, we follow the conventions of Ref. [18], where similar calculations are done for  $\chi_{c1}$ , to define the color-singlet matrix element as

$$\langle \mathcal{O}^{\chi'_{c1}}({}^3P_1^{[1]}) \rangle = \frac{9}{4\pi} |R'_{2P}(0)|^2, \quad (4)$$

where  $R'_{2P}(0)$  is the derivative of the  $\chi'_{c1}$  radial wave function at the origin, and the definition in (4) is different from that in [15] by a factor of  $1/(2N_c)$ . Similarly, we parameterize the color-octet matrix element by the ratio

$$r = m_c^2 \langle \mathcal{O}^{\chi'_{c1}}({}^3S_1^{[8]}) \rangle / \langle \mathcal{O}^{\chi'_{c1}}({}^3P_1^{[1]}) \rangle \quad (5)$$

as in Ref. [18]. Thus the cross section in (2) will be a simple function of parameters  $r$ ,  $k$  and  $|R'_{2P}(0)|^2$ . For further simplification, we fix the value of wavefunctions

$$|R'_{2P}(0)|^2 = |R'_{1P}(0)|^2 = 0.075 \text{ GeV}^5, \quad (6)$$

where in the second equality the value for  $\chi_c(1P)$  is chosen from the B-T type potential model calculation [19] and was successfully used to evaluate the cross sections of  $\chi_{c1,2}$  to account for the LHCb measurements [20], and the first equality  $|R'_{2P}(0)|^2 = |R'_{1P}(0)|^2$  is assumed based on various potential model calculations [19], and this assumption has been adopted in our previous evaluation of the ratio  $\frac{Br(B \rightarrow \chi'_{c1} K)}{Br(B \rightarrow \chi_{c1} K)}$  [9]. So it will be convenient to compare the results of  $X$  production in  $pp$  collision with that in B decay. Actually, any change of  $|R'_{2P}(0)|^2$  can be simply compensated by the corresponding change of  $k$ , and we will back to this point latter.

As for the numerical calculation, we choose the same input parameters as Ref. [18]. we use the CTEQ6L1 and CTEQ6M PDFs [21] for LO and NLO calculations respectively. The charm quark mass is set to be  $m_c = 1.5$  GeV, meanwhile the renormalization, factorization and NRQCD scales are  $\mu_r = \mu_f = \sqrt{p_T^2 + 4m_c^2}$  and  $\mu_\Lambda = m_c$ . To estimate theoretical uncertainties, we vary  $\mu_r$  and  $\mu_f$

from  $m_T/2$  to  $2m_T$  and choose  $m_c = 1.5 \pm 0.1$  GeV. We refer other details of the calculations to Ref. [18].

One should note that the  $D^0 \bar{D}^{*0}$  molecule can also be produced in  $pp$  collision through the short distance  $c\bar{c}$  pair production with small relative velocity  $v$ . Therefore, the cross section can be factorized similar to that in (3) and given by [14]

$$\sigma(D^0 \bar{D}^{*0}) = \hat{\sigma}({}^3S_1^{[1]}) \langle \mathcal{O}^{D\bar{D}^*}({}^3S_1^{[1]}) \rangle + \hat{\sigma}({}^3S_1^{[8]}) \langle \mathcal{O}^{D\bar{D}^*}({}^3S_1^{[8]}) \rangle, \quad (7)$$

where the PDFs have been integrated out in the coefficients  $\hat{\sigma}({}^3S_1^{[1,8]})$ , and the NRQCD velocity scaling rule [15] and heavy quark spin symmetry [22] have been adopted to truncate the formula to  ${}^3S_1^{[1,8]}$  terms. The coefficients  $\hat{\sigma}({}^3S_1^{[1,8]})$  are the same as those in the charmonium cross section. We evaluate them at NLO in the same scheme mentioned above, and find that the ratio  $\hat{\sigma}({}^3S_1^{[1]})/\hat{\sigma}({}^3S_1^{[8]})$  is about  $5.3 \times 10^{-4}$  for the CDF with  $p_T > 5$  GeV and  $1.5 \times 10^{-4}$  for the CMS with  $p_T > 10$  GeV (the coefficient  $\hat{\sigma}({}^3S_1^{[1]})$  has been divided by  $2N_c$  to match the convention in Ref. [14]). Note that the matrix elements in (7) are of the same order, and thus the color-singlet contributions can be neglected.

Furthermore, the matrix elements  $\langle \mathcal{O}^{D\bar{D}^*}({}^3S_1^{[1,8]}) \rangle$  for a loosely bound state should be much smaller than those of charmonia, which can be justified by the calculations of Refs. [12, 13], thus we neglect the contributions from (7) in our mixing model. However, Artoisenet and Braaten [14] argued that the  $D\bar{D}^*/\bar{D}D^*$  rescattering effects could enhance the molecule matrix elements to be consistent with the CDF data of total cross section for  $X(3872)$ . Anyway, the two models are different in different combinations of channels in (3) and in (7). Thanks to the cross section  $p_T$  distribution of  $X(3872)$  measured by CMS Collaboration [17], which allows us to compare the two different combinations in the two models.

Using formula (2) and (3), we fit the CMS  $p_T$  data ( $\sqrt{s} = 7$  TeV,  $|y| < 1.2$ ) [17] by minimizing the  $\chi^2$ , and the results are shown in Fig. 1 with the outcomes

$$r = 0.26 \pm 0.07, \quad k = 0.014 \pm 0.006, \quad (8)$$

where the central values correspond to  $\chi^2/2 = 0.26$ , and the larger error-bars, indicated by the broad band in Fig. 1, are due to the insensitivity of the  $p_T$  distribution to the parameter  $r$  in the range 0.20-0.40. Nevertheless, one can see that the central value of  $r$  in (8) is almost the same as that in Ref. [18], i.e.  $r = 0.27$ , for  $\chi_{c1}(1P)$ . This strongly suggests that  $X(3872)$  be produced through its  $\chi'_{c1}$  component at short distances. In comparison, the  $p_T$  behavior of the  ${}^3S_1^{[8]}$  channel is also shown solely in Fig. 1, which can hardly explain the data. Thus, the molecule production mechanism in (7), where the contribution from the  ${}^3S_1^{[1]}$  can be neglected as mentioned above, is disfavored by the CMS data. More explicitly, we use (7) to fit the  $p_T$  distribution and get

$$\langle \mathcal{O}^{D\bar{D}^*}({}^3S_1^{[8]}) \rangle Br_0 = 6.0 \times 10^{-5} \text{ GeV}^3, \quad \chi^2/3 = 1.03. \quad (9)$$

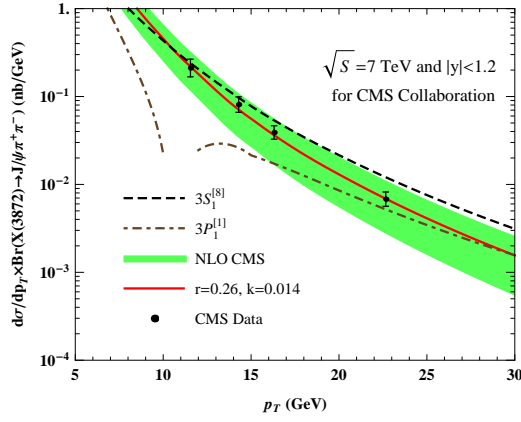


FIG. 1: The  $p_T$  distribution of prompt production cross section of  $X(3872)$ . The CMS data are taken from Ref. [17]. The theoretical curves are obtained from the two-parameter fits. The dashed, dot-dashed and solid lines represent the  $3S_1^{[8]}$ ,  $3P_1^{[1]}$  and total contributions, respectively. The green bands denoted the uncertainties of the total results.

For the CDF window ( $\sqrt{S} = 1.96$  TeV,  $|y| < 0.6$ ,  $p_T > 5$  GeV), using the central values in (8), we predict the total cross section to be

$$\sigma_{CDF}^{th}(pp \rightarrow X(J/\psi\pi^+\pi^-)) = 2.5 \pm 0.7 \text{ nb}, \quad (10)$$

which is consistent with the data in (1). Besides, since the  $p_T$  distributions of  $X(3872)$  and  $\psi'$  production are very similar both for the CMS [17] and D0 data [3], one can expect that the same case would also occur for the CDF data. Therefore, we compare our prediction for the CDF  $p_T$  distribution of  $X(3872)$  with that of  $\psi'$  [23], and the results are shown in Fig. 2, where the total cross section of  $\psi'$  has been rescaled to be the central value in (11). As for the molecule production, not only the  $3S_1^{[8]}$  dominant mechanism can not account for the  $p_T$  distribution of  $\psi'$  as shown in Fig.2, but also the predicted total cross section for CDF is too small, which can be obtained by using (7) and the matrix element in (9):

$$\sigma_{CDF}^{molecule}(pp \rightarrow X(J/\psi\pi^+\pi^-)) = 1.1 \pm 0.4 \text{ nb}, \quad (11)$$

which is about three times smaller than the CDF data in (1). This indicates that the CDF data and CMS data are consistent with each other in our model, but seem to be inharmonious in the molecule model.

For the LHCb window ( $\sqrt{S} = 7$  TeV,  $2.5 < y < 4.5$ ,  $5 \text{ GeV} < p_T < 20 \text{ GeV}$ ), using the central values in (8), we predict the total cross section to be

$$\sigma_{LHCb}^{th}(pp \rightarrow X(J/\psi\pi^+\pi^-)) = 9.4 \pm 2.2 \text{ nB}, \quad (12)$$

which is about two times larger than the experimental data [16],

$$\sigma_{tot}^{ex.}(pp \rightarrow X(J/\psi\pi^+\pi^-)) = 5.4 \pm 1.5 \text{ nB}. \quad (13)$$

One should note that in (13) about 20% of the total cross section comes from b-decays, thus our prediction in (12)

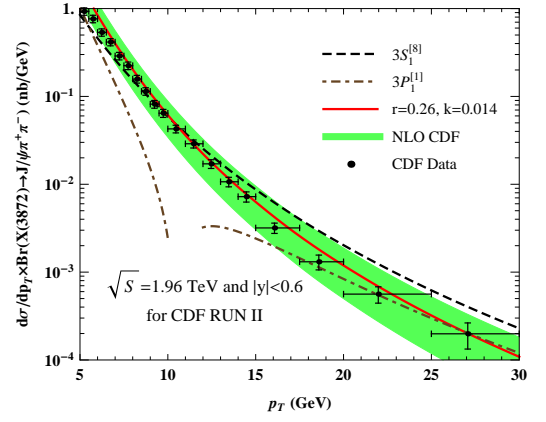


FIG. 2: Comparison between our prediction and the CDF data [23] for the  $p_T$  distribution. As mentioned in the text, the total cross section of the  $\psi'$  data has been rescaled to be the central value in (11).

is different from the LHCb data by about  $2\sigma$  deviation. However, the error-bar in (13) is larger, and we expect more available data can be used to do the analysis.

In fact, changing the values of  $r$  and  $k$  can improve our predictions, especially when the CMS  $p_T$  distribution is not sensitive to  $r$  (as mentioned above). Thus, we fix  $r$  and fit  $k$  to the CMS  $p_T$  distribution data, and the results are shown in Table I, where only the central values of  $k$  and the predicted cross sections are listed. From the Table one can see that  $\sigma_{CDF}^{th}$  and  $\sigma_{LHCb}^{th}$  have different  $r$ -dependence, and thus can not be simultaneously consistent with data in (1) and (13).

TABLE I: The one parameter fit to the CMS  $p_T$  distribution with fixed  $r$ . Only the central values of the obtained  $k$  and the predicted  $\sigma_{CDF}^{th}$  and  $\sigma_{LHCb}^{th}$  are list here.

$r$	$k$	$\chi^2/d.o.f.$	$\sigma_{CDF}^{th}(\text{nB})$	$\sigma_{LHCb}^{th}(\text{nB})$
0.20	0.021	0.39	3.26	12.2
0.25	0.015	0.17	2.63	9.87
0.30	0.012	0.20	2.28	8.56
0.35	0.010	0.27	2.06	7.72
0.40	0.008	0.34	1.90	7.14

The value of  $k$  can also be extracted from the B decay data, since in our model the branching ratio can be factorized as

$$Br(B \rightarrow X(J/\psi\pi^+\pi^-)K) = Br(B \rightarrow \chi'_{c1}K) \cdot k, \quad (14)$$

and the short distance branching ratio  $Br(B \rightarrow \chi'_{c1}K)$  can be extracted by fitting the line shape of the experimental curves [24, 25]. With a reasonable choice of the decay width of  $X(3872)$ , the fit in Ref. [25] gives

$$Br^{fit}(B \rightarrow \chi'_{c1}K) = (3.7 - 5.7) \times 10^{-4}, \quad (15)$$

which is consistent with our prediction in [9]. By com-

paring (14) and (15) with

$$Br(B \rightarrow X(J/\psi\pi^+\pi^-)K) = (8.6 \pm 0.8) \times 10^{-6} \quad [5], \quad (16)$$

the constraints on  $k$  from B decay is given by

$$k = 0.018 \pm 0.004, \quad (17)$$

which is consistent with our fits to the CMS  $p_T$  distribution for  $r = 0.20$ - $0.26$  in Table I, and thus consistent with the CDF data but not the LHCb data.

As for the value of  $|R'_{2P}(0)|^2$ , if one choose a larger one than that in (6), say,  $0.102 \text{ GeV}^5$  [19], the value of  $k$  in Table I will be decreased by a factor of 0.75 with fixed  $r$ , and the overlap between Table I and (17) tends to disappear. Thus, our fits disfavor the larger one.

Finally, with a modest value  $Br_0 = 0.05$  which satisfies the experimental constraints [5], the window of  $k$  in (17) will correspond to the probability of  $\chi'_{c1}$  component in the  $X(3872)$ :

$$Z_{c\bar{c}} = (28\text{-}44)\%, \quad (18)$$

which is consistent both with our original arguments and with the fits in Ref. [25].

*Summary.*—Within the framework of NRQCD factorization, we evaluate the cross sections of  $X(3872)$  at the Tevatron and LHC at NLO in  $\alpha_s$  by assuming that the

short distance production proceeds dominantly through its  $\chi'_{c1}$  component. The fit of the CMS  $p_T$  distribution data [17] gives the ratio  $r = 0.26 \pm 0.07$ , which is almost the same as that for  $\chi_{c1}$  [18], and strongly supports the  $\chi'_{c1}$  dominant production mechanism for  $X(3872)$ . The outcomes of the fits can well account for the CDF data [2, 13], and are consistent with the value of  $k = Z_{c\bar{c}} \cdot Br_0$  constrained by the B decay data simultaneously. The predicted cross section for the LHCb is larger than the data [16] by a factor of 2, which might be due to the large theoretical and experimental uncertainties. We also evaluate the cross section of the  $D^0\bar{D}^{*0}$  molecule [14] at NLO, and find that the molecule dominant production mechanism for  $X(3972)$  is inconsistent with both the  $p_T$  distributions and the total cross sections of the CMS and CDF data.

We thank J.Z. Li, Y.Q. Ma and Y.J. Zhang for helpful discussions. This work was supported in part by the National Natural Science Foundation of China (No 11075002, No 11021092), and the Ministry of Science and Technology of China (2009CB825200).

*Note :* When this work was prepared, there appeared another paper [26] to study the prompt production of  $X(3872)$  as the  $\chi'_{c1}$  meson. Though some of their results are similar to ours, we put stress on the  $\chi'_{c1} - D^0\bar{D}^{*0}$  mixing model proposed in [9], and find the  $\chi'_{c1}$  component in  $X(3872)$  can be dominant if  $Br(X \rightarrow J/\psi\pi^+\pi^-) < 0.04$ .

- 
- [1] S. K. Choi *et al.* (Belle Collaboration), Phys. Rev. Lett. **91**, 262001 (2003).
  - [2] D. Acosta *et al.* (CDF II Collaboration), Phys. Rev. Lett. **93**, 072001 (2004).
  - [3] V. M. Abazov *et al.* (D0 Collaboration), Phys. Rev. Lett. **93**, 162002 (2004).
  - [4] B. Aubert *et al.* (BaBar Collaboration), Phys. Rev. D **71**, 071103 (2005).
  - [5] J. Beringer *et al.* (Particle Data Group), Phys. Rev. D **86**, 010001 (2012).
  - [6] N.A. Tornqvist, Phys. Lett. B **590**, 209 (2004); F. Close and P. Page, Phys. Lett. B **578**, 119(2004); C.Y. Wong, Phys. Rev. C **69**, 055202 (2004); M.B. Voloshin, Phys. Lett. B **604**, 69 (2004); E. Swanson, Phys. Lett. B **588**, 189 (2004); E. Braaten, M. Kusunoki and S. Nussinov, Phys. Rev. Lett. **93**, 162001 (2004).
  - [7] N. Brambilla *et al.*, Eur. Phys. J. C **71**, 1534 (2011).
  - [8] A. Tomaradze *et al.*, arXiv:1212.4191[hep-ex].
  - [9] C. Meng, Y.J. Gao and K.T. Chao, arXiv:hep-ph/0506222, to appear in PRD.
  - [10] C. Meng and K.T. Chao, Phys. Rev. D **75**, 114002 (2007).
  - [11] B.Q. Li, C. Meng and K.T. Chao, Phys. Rev. D **80**, 014012 (2009); I.V. Danilkin and Yu.A. Simonov, Phys. Rev. Lett. **105**, 102002 (2010).
  - [12] M. Suzuki, Phys. Rev. D **72**, 114013 (2005).
  - [13] C. Bignamini *et al.*, Phys. Rev. Lett. **103**, 162001 (2009).
  - [14] P. Artoisenet and E. Braaten, Phys. Rev. D **81**, 114018 (2010).
  - [15] G.T. Bodwin, E. Braaten and E.P. Lepage, Phys. Rev. D **51**, 1125 (1995); **55**, 5853(E) (1997).
  - [16] R. Aaij *et al.* (LHCb Collaboration), Eur. Phys. J. C **72**, 1972 (2012).
  - [17] S. Chatrchayan *et al.* (CMS Collaboration), arXiv:1302.3968[hep-ex].
  - [18] Y.-Q. Ma, K. Wang and K.-T. Chao, Phys. Rev. D. **83**, 111503 (2011).
  - [19] E. J. Eichten and C. Quigg, Phys. Rev. D **52**, 1726 (1995).
  - [20] R. Aaij *et al.* (LHCb Collaboration), Phys. Lett. B **718**, 431 (2012).
  - [21] M.R. Whalley, D. Bourilkov and R.C. Group, arXiv:hep-ph/0508110.
  - [22] M.B. Voloshin, Phys. Lett. B **604**, 69 (2004).
  - [23] T. Aaltonen *et al.* (CDF Collaboration), Phys. Rev. D **80**, 031103(R) (2009).
  - [24] O. Zhang, C. Meng and H.Q. Zheng, Phys. Lett. B **680**, 453 (2009);
  - [25] Yu.S. Kalashnikova and A.V. Nefediev, Phys. Rev. D **80**, 074004 (2009).
  - [26] M. Butenschoen, Z.G. He and B.A. Kniehl, arXiv:1303.3524[hep-ph]